

SUPPLEMENTAL MATERIAL

Materials and Methods

Animals and Diet

Male apoE^{-/-} mice, LDb (Ldlr^{-/-}Apobec1^{-/-}) mice,¹ TLR4^{-/-} mice (all on a C57BL/6 background) and C57BL/6 wild-type (WT) mice, CD11c^{-/-}/apoE^{-/-} and CD11c^{+/+}/apoE^{-/-} littermates,² CD36^{obl/obl} mice³ (deficient in functional CD36 and on a C57BL/6 background; obtained through Mutant Mouse Regional Resource Centers) and CD36^{+/+} WT littermate controls were used. ApoE^{-/-} mice, TLR4^{-/-} mice and C57BL/6 mice were originally purchased from the Jackson Laboratory (Bar Harbor, ME) and the mouse colonies were maintained in a pathogen-free animal facility of Baylor College of Medicine. Mice were either maintained on normal chow diet (ND, PicoLab Rodent Chow 5010; LabDiet, St. Louis, MO) throughout, or switched to western high-fat diet (WD) (21% milkfat [w/w], 0.2% cholesterol [w/w]; Dyets Inc., Bethlehem, PA) at the age of 8 weeks and maintained on WD for up to 10 weeks, or switched to a high-fat low-cholesterol diet (HFD) (21% milkfat [w/w], 0.05% cholesterol [w/w]; Dyets Inc.) or low-fat high-cholesterol diet (HCD) (5% milkfat [w/w], 0.2% cholesterol [w/w]; Dyets Inc.) at the age of 8 weeks and maintained on these diets for 2 weeks. A total of 346 male mice, including 116 “WT,” 170 apoE^{-/-}, 5 LDb, 12 CD36^{obl/obl}, 3 TLR4^{-/-}, 20 CD11c^{+/+}/apoE^{-/-} and 20 CD11c^{-/-}/apoE^{-/-}, were used. All mice were housed in a pathogen-free facility that maintained a 12-hour light/12-hour dark cycle. Blood was drawn via retro-orbital puncture, and plasma total cholesterol and triglyceride levels were measured using enzymatic procedures with Wako products (Wako Diagnostics, Richmond, VA). All animal studies were approved by the Institutional Animal Care and Use Committee of Baylor College of Medicine.

Antibodies and flow cytometric (FACS) analysis of blood and aortas

The following monoclonal antibodies (mAbs) to mouse antigens, with appropriate isotype negative controls, were used: CD45 (FITC-conjugated), CD11c (FITC-, PE- or PerCP-Cy5.5-conjugated), CD11b (FITC-conjugated), Ly-6C (FITC- or APC-conjugated) (BD Biosciences, San Jose, CA); CD115 (PE-conjugated), F4/80 (FITC- or PerCP-Cy5.5-conjugated) (eBioscience, San Diego, CA); CD204 (FITC-conjugated), and CD36 (FITC-conjugated) (AbD Serotec Inc., Raleigh, NC).

For FACS analysis of blood, blood was drawn through retro-orbital puncture. After dilution with equal volume of PBS supplemented with 0.5% BSA, whole blood was incubated with various combinations of fluorescence-conjugated mAbs as described in Results or with appropriate isotype negative controls for 20 min. Then, the samples were washed once with PBS, incubated with BD FACS Lysing Solution (BD Biosciences) for 10 min to lyse red blood cells, and washed another time with PBS. In some cases, after lysing red blood cells, the samples were stained with Nile red using Lipid Droplets Fluorescence Assay Kit (Cayman Chemical Company, Ann Arbor, MI). Finally, the stained cells were resuspended in 1% paraformaldehyde in PBS. Data were collected with a BD FACScan or LSRII flow cytometer (BD Biosciences) and analyzed with FlowJo software (Tree Star Inc., Ashland, OR). Total leukocytes were gated based on scatter pattern (forward scatter [FSC] vs. side scatter [SSC]) and data were expressed as percentages of positive cells in total leukocytes or monocytes as indicated in Results. In some cases, data were analyzed in specific gated regions as described previously² and in Results. Based on the overlapping expression of CD115 and CD204,² and to minimize the numbers of

fluorophore-conjugated antibodies used, we defined mouse total monocytes as PE-CD115⁺ or FITC-CD204⁺ leukocytes, depending on the commercial availability of fluorophore choices for other markers simultaneously examined. To examine the 3 major monocyte subsets in mice (see Results), we used the combination of PE-anti-CD115 + FITC-anti-CD36 + PerCP-Cy5.5-anti-CD11c antibodies. To examine Ly-6C expression on the 3 monocyte subsets, we used the combination of PE-anti-CD115 + FITC-anti-CD36 + PerCP-Cy5.5-anti-CD11c + APC-anti-Ly-6C antibodies.

For FACS analysis of mouse aortas, mice were sacrificed and perfused with PBS containing 20 U/ml of heparin, and whole aortas, from 2 mm distal to the heart to just beyond the renal artery, were dissected from mice and cleared of all adipose tissue under a dissection microscope.² The dissected aortas were weighed to control the total amount of collected aortic tissues, and then were minced and digested with 125 U/ml collagenase type XI, 60 U/ml hyaluronidase type I, 60 U/ml DNase I, and 450 U/ml collagenase type I (Sigma-Aldrich) in PBS containing 20 mM HEPES at 37°C for 1 hour.⁴ Cell suspension was obtained by pressing the aorta through a 70- μ m strainer. After being washed with PBS twice, cells were incubated with Mouse BD Fc Block (BD Biosciences) at 4°C for 5 min, then incubated with mAbs or negative isotype controls and viability dye (eBioscience) for 20 min at 4°C, then washed with PBS twice more. Data were collected with a BD LSRII flow cytometer and analyzed using FlowJo software. Cells were first gated based on FSC and SSC pattern, then viable cells were analyzed for CD45 expression. Data are presented as percentages of targeted cell populations in viable CD45⁺ cells of aortic cell suspensions.^{4, 5} For this assay, each sample included aortas pooled from 2–3 mice of the same strain.

Monocyte uptake of cholesterol ester–rich very-low-density lipoproteins (CE-VLDLs)

CE-VLDLs were isolated from plasma of apoE^{-/-} mice on WD by ultracentrifugation⁶ and labeled with DiI by incubation at room temperature for 30 min with subsequent overnight dialysis in PBS. CE-VLDL oxidation was estimated by malondialdehyde levels (TBARS value) as measured using TBARS assay kit (Cayman Chemical, Ann Arbor, MI). DiI-CE-VLDLs were stored at 4°C and used within 2 weeks. To examine monocyte uptake of CE-VLDLs, a bolus of DiI-CE-VLDLs, at 75 μ g cholesterol/g body weight, was injected intravenously (and in some cases, intraperitoneally) into mice. At 3 and 24 hours postinjection, blood was collected via retro-orbital puncture, and monocyte uptake of CE-VLDLs and phenotypic changes were examined by flow cytometry.² As a control, a bolus of free DiI was injected intravenously into mice, and monocytes were examined by flow cytometry at 3 and 24 hours postinjection.

Monocyte isolation

Blood was collected by cardiac puncture from apoE^{-/-} mice on WD under deep anesthesia. Mononuclear cells (MNCs) were first isolated from whole blood using Histopaque 1083 (Sigma-Aldrich, St. Louis, MO). Total monocytes were then purified from MNCs using a customized EasySep Mouse Monocyte Enrichment Kit (Stemcell Technologies, Vancouver, BC). CD11c-conjugated microbeads (Miltenyi Biotec, Bergisch Gladbach, Germany) were used to separate total monocytes into CD11c⁺ foamy monocytes and CD11c⁻ nonfoamy monocytes.² CD11c⁺ and CD11c⁻ monocytes were dissolved in Trizol reagent (Life Technologies, Carlsbad, CA) for RNA isolation.

EdU injection

Mice were injected intraperitoneally with a bolus of EdU (Life Technologies) at 4 $\mu\text{g/g}$ body weight. Blood was collected through retro-orbital puncture at various time points as indicated in Results and stained for EdU using Click-iT® EdU Flow Cytometry Assay Kit (Life Technologies).⁷ EdU⁺ monocytes, which represented newly released monocytes from bone marrow, were phenotyped for CD11c and CD36 expression by flow cytometry.

Tissue culture with THP1 monocytes

THP1 monocytes (ATCC, Manassas, VA) were cultured and grown in RPMI-1640 medium supplemented with 10% fetal bovine serum, 0.05 mM 2-mercaptoethanol and penicillin/streptomycin. For experiments, THP1 monocytes were switched to RPMI-1640 medium supplemented with 0.05 mM 2-mercaptoethanol and penicillin/streptomycin, and maintained in this medium for 14 hours (overnight). Then, the cells were treated with CE-VLDLs (isolated from apoE^{-/-} mice on WD), at 300 mg/dl cholesterol, or PBS (control) in serum-free medium for 48 hours. After this, THP1 monocytes were examined by flow cytometry for lipid accumulation indicated by SSC intensity and Nile red staining, and for CD36 expression after staining with an FITC-anti-human CD36 antibody (BD Biosciences) or a FITC-isotype control. To examine effects of CE-VLDL treatment on monocyte further uptake of DiI-CE-VLDL, THP1 monocytes were pretreated with (unlabeled) CE-VLDLs or PBS for 48 hours as described above. Following this, the cells were washed twice with PBS and then incubated with DiI-CE-VLDLs in serum-free medium for an additional 4 hours. Monocyte uptake of DiI-CE-VLDLs was examined by flow cytometry.

Monocyte depletion

To deplete total monocytes, a bolus of clodrosome (Encapsula NanoSciences LLC, Nashville, TN) was intravenously injected into mice at 0.3 ml/mouse. At the time points indicated in Results, blood was collected, and appearance and phenotypes of newly released monocytes were examined by flow cytometry.

In separate experiments, after WD for 3 days, apoE^{-/-} mice received daily intravenous injections of clodrosome at 0.1 ml/mouse after 1:5 dilution in PBS for an additional 3 weeks, during which mice were maintained on WD. A control group of apoE^{-/-} mice was injected with PBS at 0.1 ml/mouse and maintained on WD. At 24 hours after the final injection of clodrosome, mice were sacrificed. Hearts and whole aortas were collected for analysis of atherosclerosis development and macrophage/DC contents in atherosclerotic lesions/aortas as described in the following sections.

To examine monocyte uptake of clodrosome, a bolus of DiI-clodrosome (Encapsula NanoSciences LLC), at the doses indicated in Results, was injected intravenously into apoE^{-/-} mice that had been on WD for 3 weeks. At 3 hours postinjection, blood was collected via retro-orbital puncture and stained with FITC-anti-mouse CD204 antibody. Monocyte uptake of DiI-clodrosome was examined by flow cytometry.

Foamy monocyte infiltration into atherosclerotic lesions

A bolus of DiI-CE-VLDLs and/or 0.5 μm Fluoresbrite FITC-dyed (YG) plain microspheres (Polysciences Inc., Warrington, PA) (1:5 dilution with PBS)^{8, 9} was injected intravenously into apoE^{-/-} or CD11c^{-/-} apoE^{-/-} mice and their CD11c^{+/+} apoE^{-/-} littermate controls at day 16 on WD. At 3, 24 and 120 hours after injection, blood was collected through retro-orbital puncture, and

monocyte labeling and phenotypes were examined by flow cytometry. This procedure allowed us to label foamy monocytes specifically, with few nonfoamy monocytes labeled, in these mice (see Results). At 120 hours postinjection, mice were sacrificed, and whole aortas were dissected and digested as described above. Foamy monocytes that infiltrated into atherosclerotic aortas were identified as DiI⁺F4/80^{low} cells in viable CD45⁺ cells of aortic cell suspension as examined by flow cytometry. For comparison between CD11c^{-/-}apoE^{-/-} and CD11c^{+/+}apoE^{-/-} mice, percentages of infiltrated foamy monocytes in aortic viable CD45⁺ cells were normalized by the average proportions of DiI⁺ foamy monocytes in blood of the same mouse at the time points indicated.

Mouse hearts were also harvested, embedded in OCT (Triangle Biomedical Sciences, Durham, NC) and stored at -80°C. To examine infiltration of foamy monocytes into aortic sinus atherosclerotic lesions, serial 5-µm transverse cryosections of aortic sinus that showed all 3 aortic valves were prepared. In each mouse, ~20 consecutive sections starting from the first section to show all 3 aortic valves were prepared and numbered 1–20. Slides were stained with DAPI (Molecular Probes Inc., Eugene, OR): after equilibrating briefly with PBS, the samples were incubated with DAPI for 5 min and then rinsed several times in PBS and dried before mounting with VectaMount AQ Aqueous Mounting Medium (Vector Laboratories Inc., Burlingame, CA). The samples were viewed using an EVOS fl Fluorescence Microscope (Life Technologies) with appropriate filters. For quantification and comparison of foamy monocyte infiltration into aortic sinus lesions, 5 aortic sinus sections (numbers 1, 5, 10, 15 and 20) from each mouse were used. The DiI⁺bead⁺ cells, which represented infiltrated monocytes, were counted in each lesion section. Data are presented as average numbers of infiltrated monocytes per lesion section normalized by the proportions of DiI⁺bead⁺ foamy monocytes in blood of each mouse.^{8,9}

Analysis of atherosclerotic lesions in aortic sinus

To examine and quantify atherosclerotic lesions in aortic sinus and macrophages/DCs in the lesions, serial transverse cryosections (~20 sections/mouse) of aortic sinus that included all 3 aortic valves were made. Five sections (numbers 1, 5, 10, 15 and 20) from each mouse were stained with oil red O as described previously.² Another five sections (numbers 2, 6, 11, 16 and 19) from each mouse were stained for CD11b and CD11c.² Briefly, after blocking with 1% BSA for 30 min, sections were stained with PE-conjugated anti-mouse CD11c and/or FITC-conjugated anti-mouse CD11b mAbs by coincubation overnight at 4°C. After washing, the sections were stained for nuclei with DAPI and viewed with an EVOS fl Fluorescence Microscope. In a separate experiment, macrophage content was examined in aortic sinus atherosclerotic lesions by immunohistochemistry staining for Mac-3.² The size of atherosclerotic lesions, indicated by oil red O staining, the quantitation of CD11c⁺ macrophages/DCs, indicated by staining for CD11c, and the quantitation of Mac-3⁺ macrophages, indicated by staining for Mac-3, were calculated in each section using Image J software (NIH, Bethesda, MD) and the mean lesion size or areas positive for CD11c or Mac-3 per section are presented.

Quantitative reverse transcriptase polymerase chain reaction

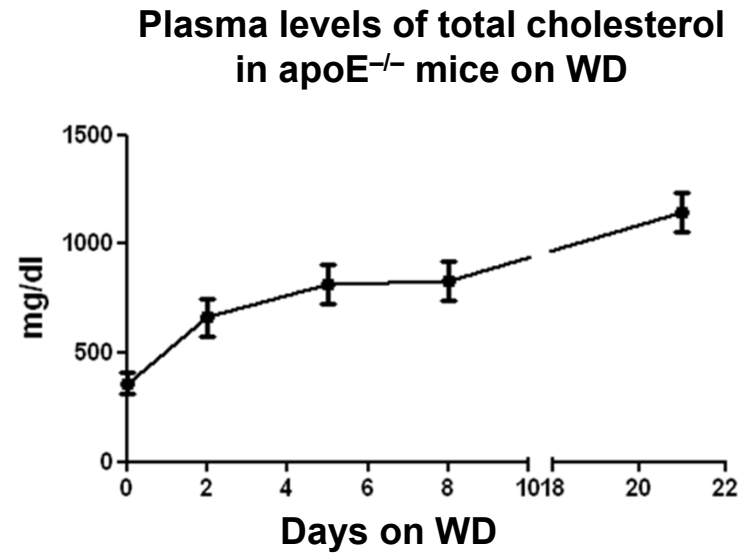
Total RNA was extracted using Trizol reagent from isolated monocytes or whole aortas, which were collected from mice and stored in RNAlater solution (Life Technologies). The relative mRNA quantities of target molecules were examined by quantitative reverse transcriptase polymerase chain reaction (RT-PCR) using predesigned primers and probes from Applied

Biosystems and normalized to that of 18S ribosomal RNA.⁷

Statistics

GraphPad Prism 5.04 (GraphPad Software, Inc., La Jolla, CA) was used for statistical analyses. Values are presented as mean±SEM. For statistical analyses, Mann–Whitney tests (for comparison between 2 groups) or Kruskal–Wallis tests (for comparisons of 3 or more groups) followed by Dunn’s multiple pairwise comparison test were used. Differences were considered significant for P values ≤0.05.

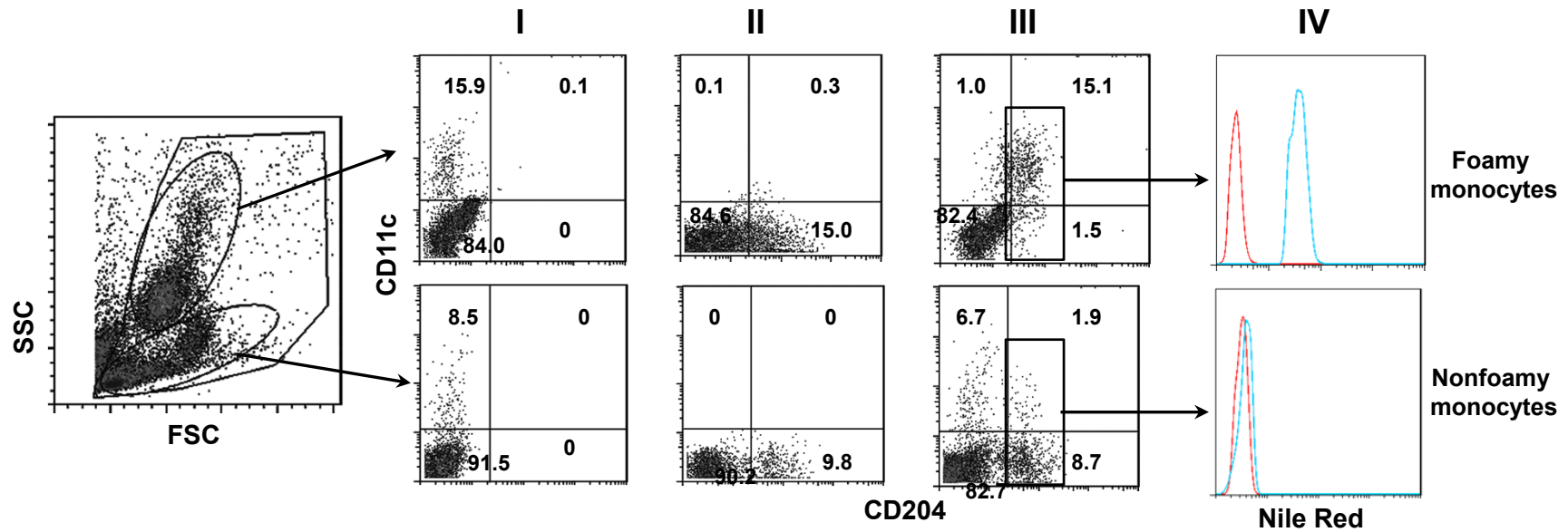
Supplemental Figure I



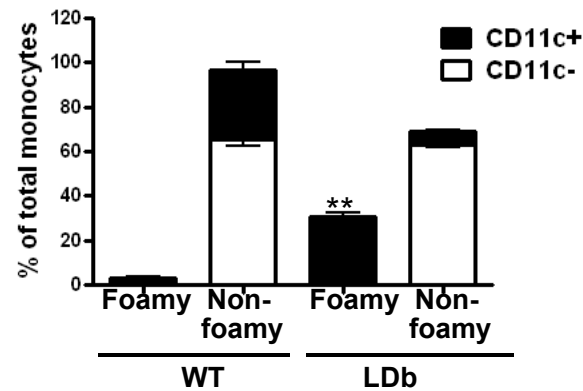
Supplemental Figure I. Plasma levels of total cholesterol in apoE^{-/-} mice at various time points on WD. n=7 mice.

Supplemental Figure II

Foamy monocytes in blood of LDb mice on WD



Monocytes in blood of LDb and WT on HFD

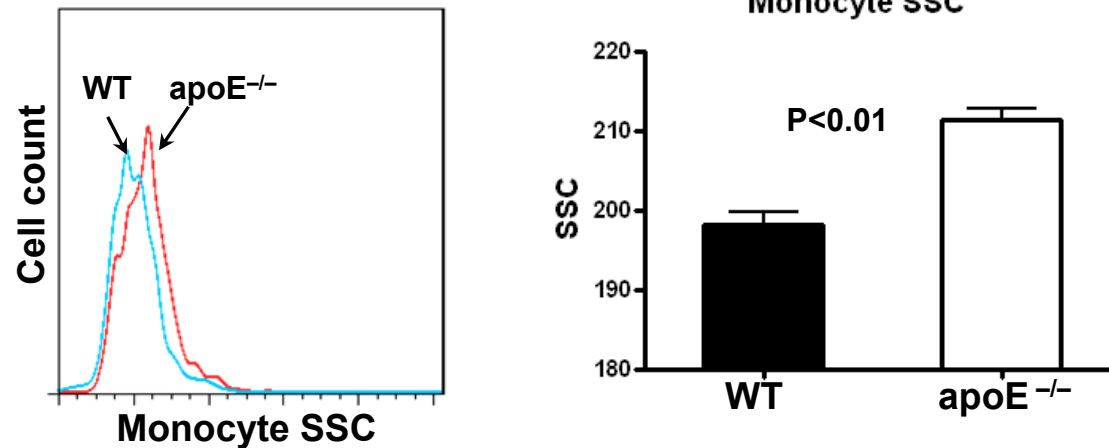


***P<0.001 vs. WT, n=5/group.

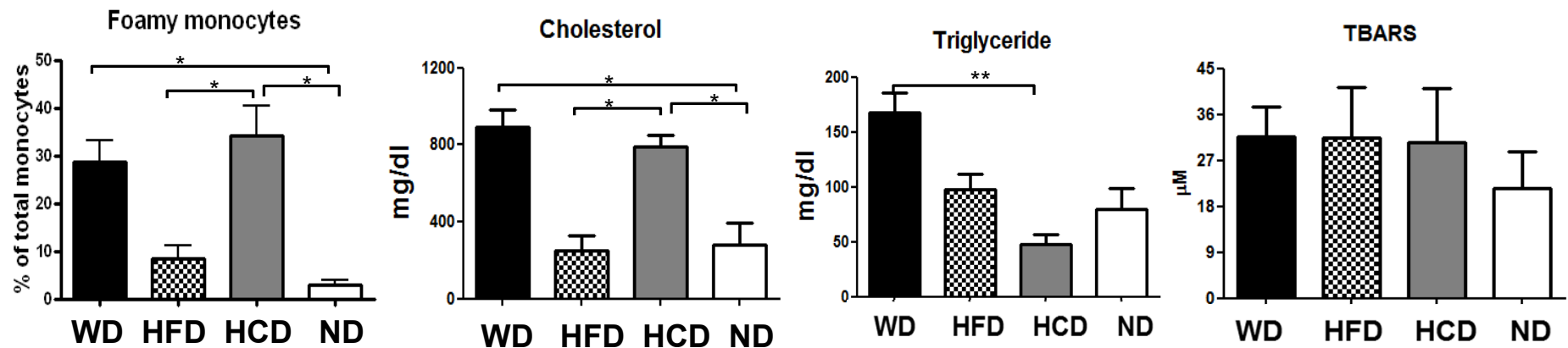
Supplemental Figure II. Monocytes in blood of LDb mice on WD (2 weeks) examined by flow cytometry. Upper panels: representative flow cytometric analysis of foamy and nonfoamy monocytes in blood of LDb mice (see Figure 1B for representative WT control) on WD with staining for: I, CD11c and negative control for CD204; II, CD204 and negative control for CD11c; III, CD11c and CD204; and IV, Nile Red. Lower panel: relative ratios of CD11c⁺ and CD11c⁻ foamy and nonfoamy monocytes in blood of WT and LDb mice on WD.

Supplemental Figure III

A. Monocyte SSC values in apoE^{-/-} mice and WT mice on ND

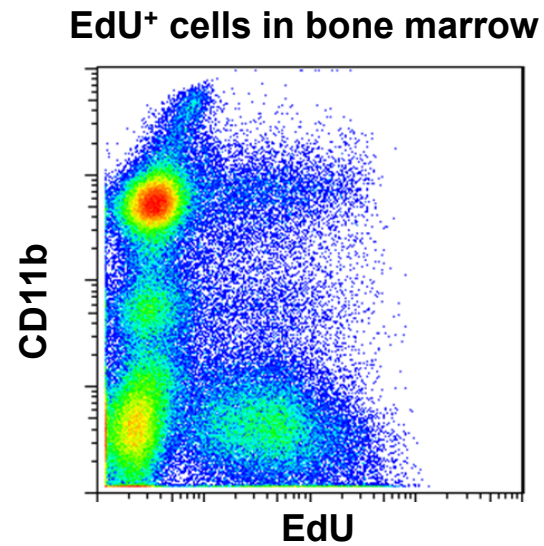


B. Foamy monocytes and lipid levels in blood of apoE^{-/-} mice on various types of diet



Supplemental Figure III. Monocytes in blood of apoE^{-/-} mice on various types of diet. A. SSC values of blood monocytes in 28-week-old apoE^{-/-} mice and WT mice on ND as examined by flow cytometry. n=6–7 mice/group. B. Proportions of foamy monocytes and levels of cholesterol, triglyceride and TBARS in blood of apoE^{-/-} mice on various types of special diet for 2 weeks. n=3–6 mice/group.

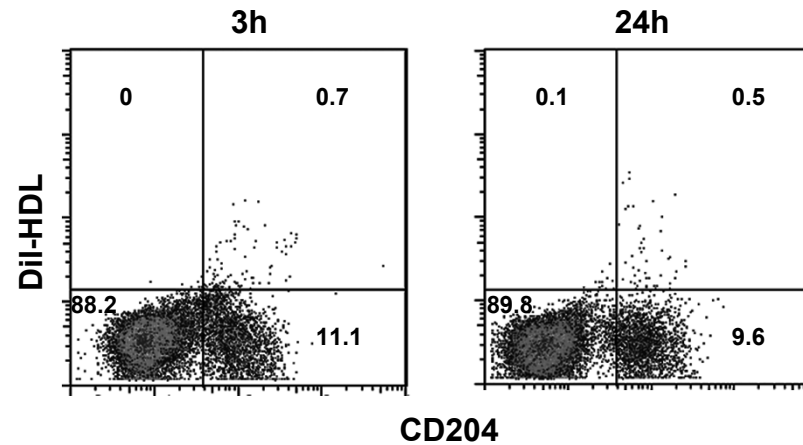
Supplemental Figure IV



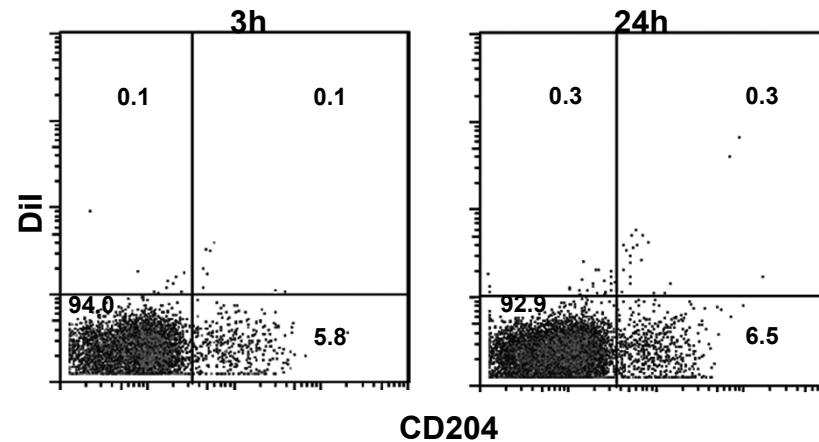
Supplemental Figure IV. A representative flow cytometric analysis showing EdU⁺ cells in bone marrow of WT mice at 3 hours after EdU injection.

Supplemental Figure V

Uptake of Dil-HDL by blood monocytes

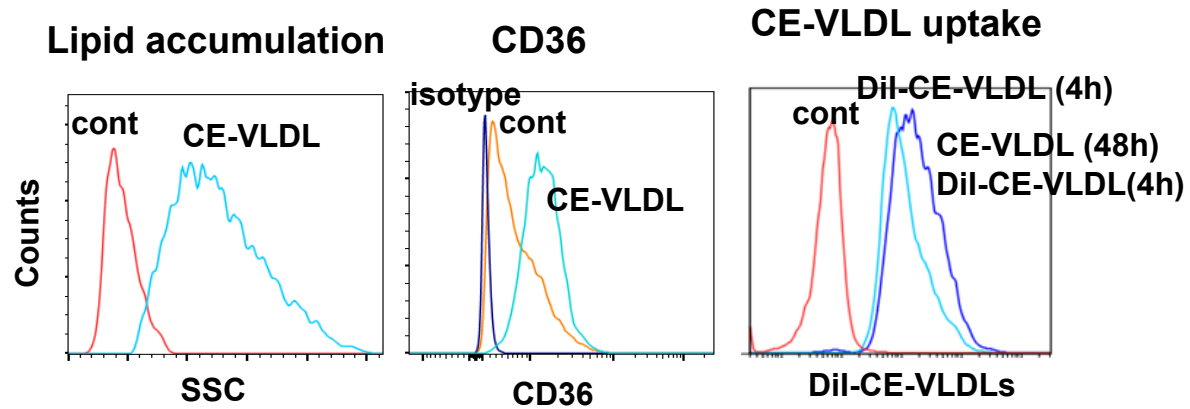


Blood monocytes after injection of free Dil



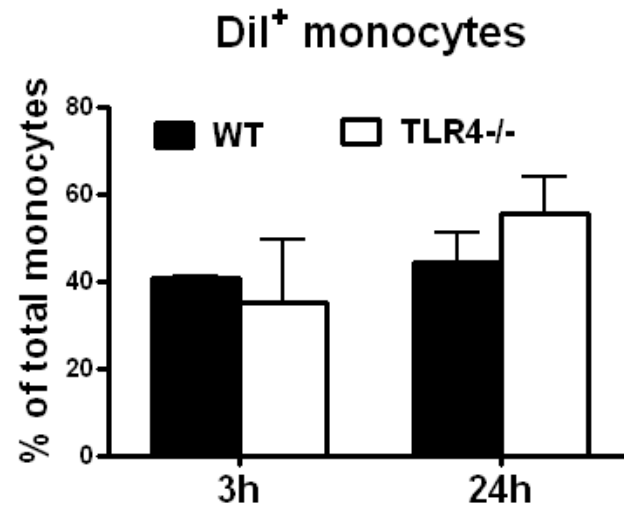
Supplemental Figure V. Flow cytometric analysis of blood monocytes in WT mice after intravenous injection of a bolus of Dil-HDL (upper panels) or free Dil (lower panels). Representatives of 3–4 mice in each condition with similar results are shown.

Supplemental Figure VI



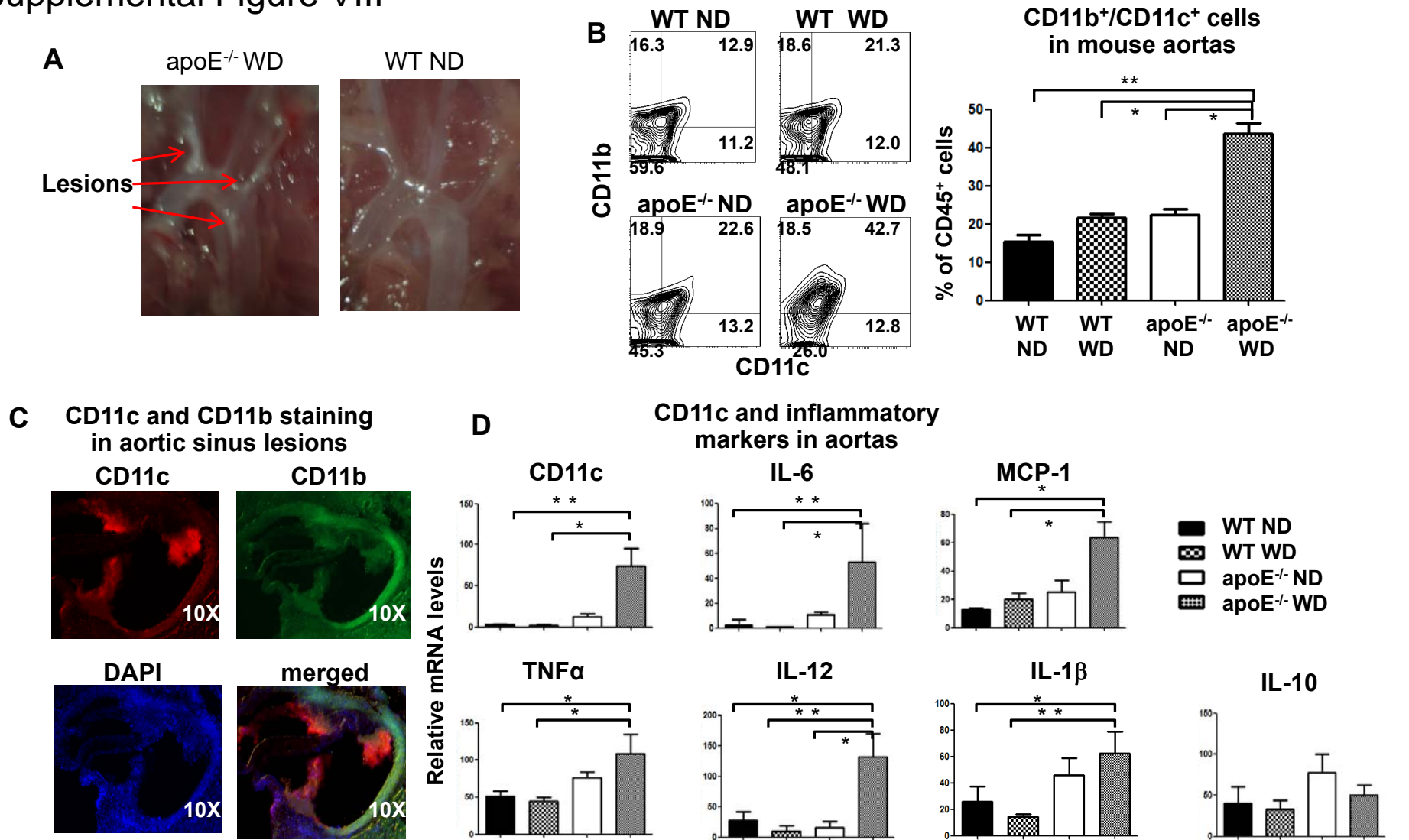
Supplemental Figure VI. Effects of CE-VLDLs on THP1 monocytes in vitro. THP1 monocytes were treated with (unlabeled) CE-VLDLs (isolated from apoE^{-/-} mice on WD), at 300 mg/dl cholesterol, or PBS (cont) for 48 hours and examined for lipid accumulation indicated by SSC change (left panel) and for CD36 expression (middle panel). For DiI-CE-VLDL uptake (right panel), THP1 monocytes were pretreated with (unlabeled) CE-VLDLs or PBS for 48 hours followed by removal of the CE-VLDLs and incubated with DiI-CE-VLDLs for an additional 4 hours. Then monocyte uptake of DiI-CE-VLDLs was examined by flow cytometry. Data were representatives from 3 independent experiments with similar results.

Supplemental Figure VII



Supplemental Figure VII. Uptake of Dil-CE-VLDLs by blood monocytes of WT and TLR4^{-/-} mice after intravenous injection of a bolus of Dil-CE-VLDLs. n=3 mice/group.

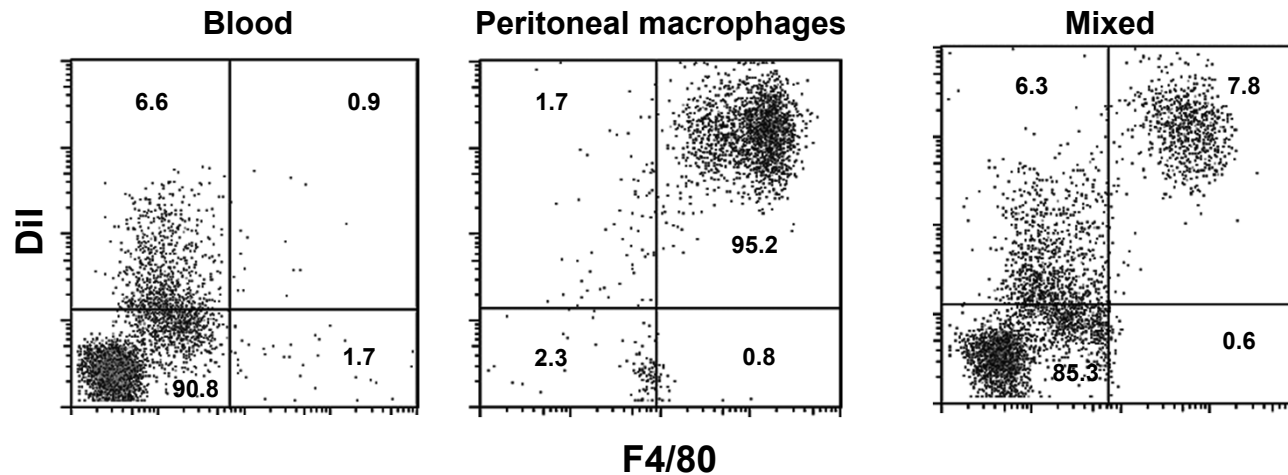
Supplemental Figure VIII



Supplemental Figure VIII. Early development of atherosclerosis and increased inflammation in atherosclerotic aortas in apoE^{-/-} mice on WD (3 weeks). **A**, Representatives of atherosclerotic plaques in aortic arch of an apoE^{-/-} mouse on WD and a WT (on ND). **B**, CD11b⁺/CD11c⁺ cells in mouse aortas quantified by flow cytometry. n=3–4 samples/group. **C**, Representative immunofluorescent staining for CD11c (red) and CD11b (green) in aortic sinus sections of apoE^{-/-} mice on WD. **D**, mRNA levels of CD11c and inflammatory markers in mouse aortas. n= 5–10 mice/group. *P<0.05, **P<0.01.

Supplemental Figure IX

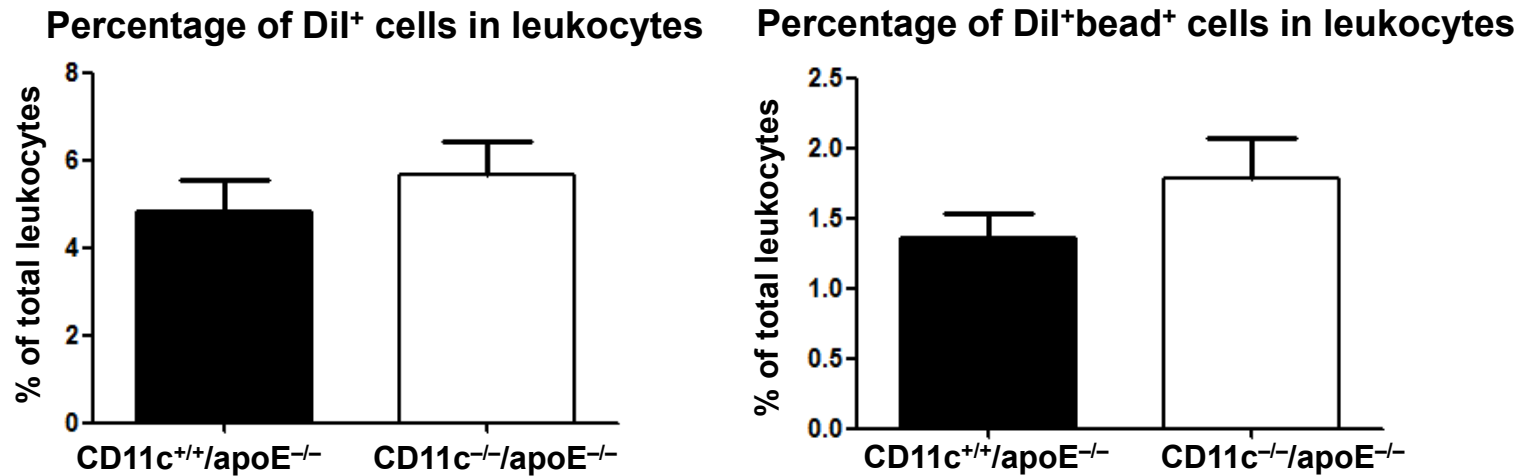
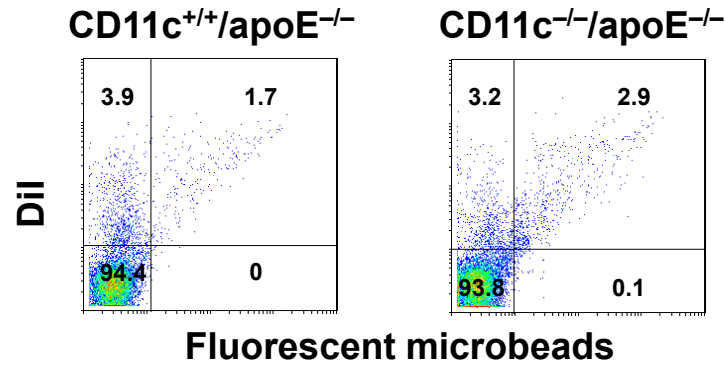
F4/80 expression on Dil-CE-VLDL-labeled blood monocytes and peritoneal macrophages



Supplemental Figure IX. A bolus of Dil-CE-VLDLs was injected intravenously and intraperitoneally into apoE^{-/-} mice on WD (3 weeks). At 24 hours after injection, blood monocytes and peritoneal macrophages were collected and stained for F4/80 separately or blood and peritoneal cells were mixed and then stained for F4/80. The data shown were representatives from 3 mice with similar results and showed higher F4/80 levels on peritoneal macrophages than blood monocytes. However, the Dil(-CE-VLDL) levels were not comparable between peritoneal macrophages and blood monocytes in our models given that once intravenously injected, Dil-CE-VLDLs circulated in blood and were diluted quickly, whereas after intraperitoneal injection, Dil-CE-VLDLs stayed “static” and may also have been more concentrated in the peritoneal cavity, thereby leading to “longer” interaction of peritoneal macrophages with Dil-CE-VLDLs in the peritoneal cavity, which may explain the higher Dil levels on peritoneal macrophages.

Supplemental Figure X

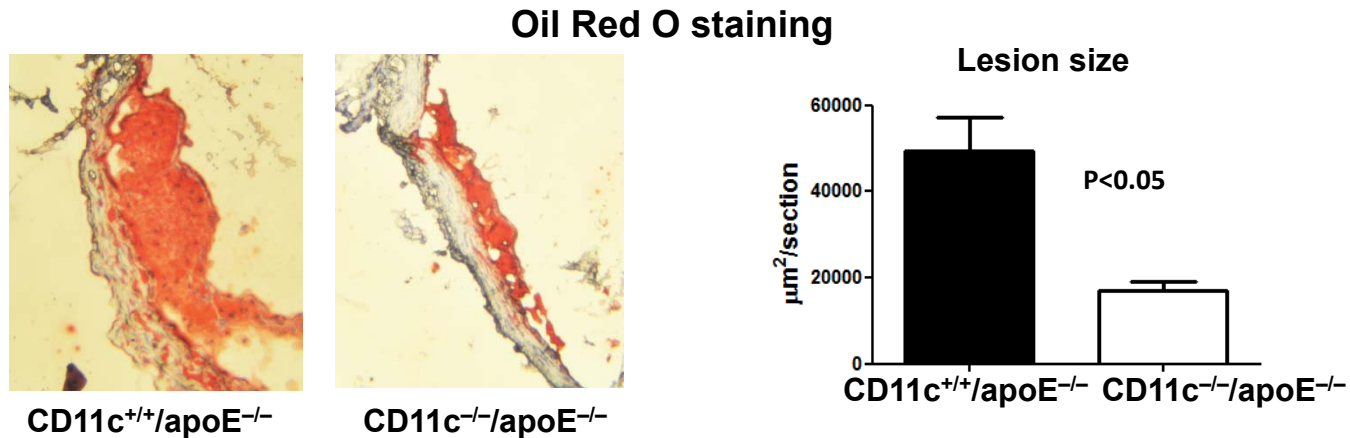
Dil⁺/bead⁺ monocytes in blood of CD11^{+/+}/apoE^{-/-} and CD11c^{-/-}/apoE^{-/-} mice



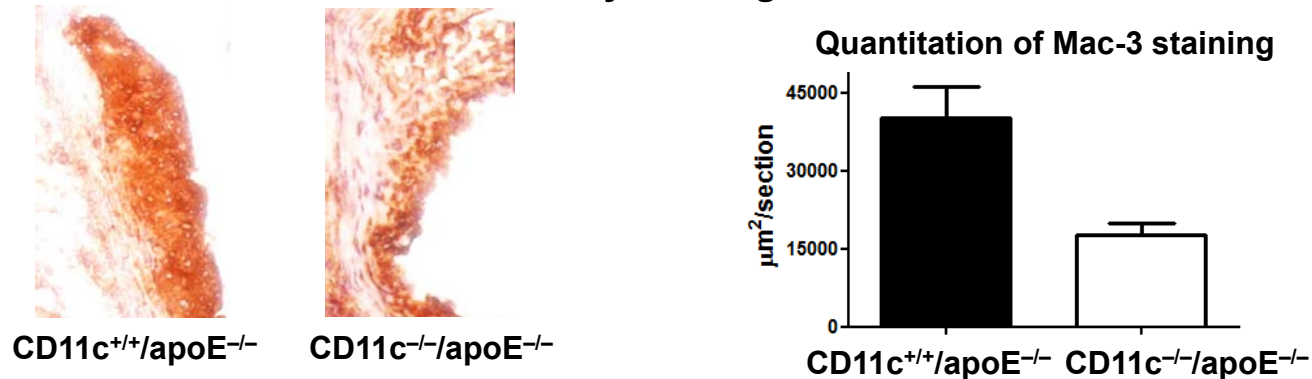
Supplemental Figure X. CD11c^{+/+}/apoE^{-/-} and CD11c^{-/-}/apoE^{-/-} mice on WD (3 weeks) were injected intravenously with Dil-CE-VLDLs and fluorescent microbeads. At 24 hours after injection, blood was collected and uptake of Dil-CE-VLDLs and fluorescent microbeads by blood monocytes was examined by flow cytometry.

Supplemental Figure XI

Atherosclerotic lesions and macrophages in CD11^{+/+}/apoE^{-/-} and CD11c^{-/-}/apoE^{-/-} mice



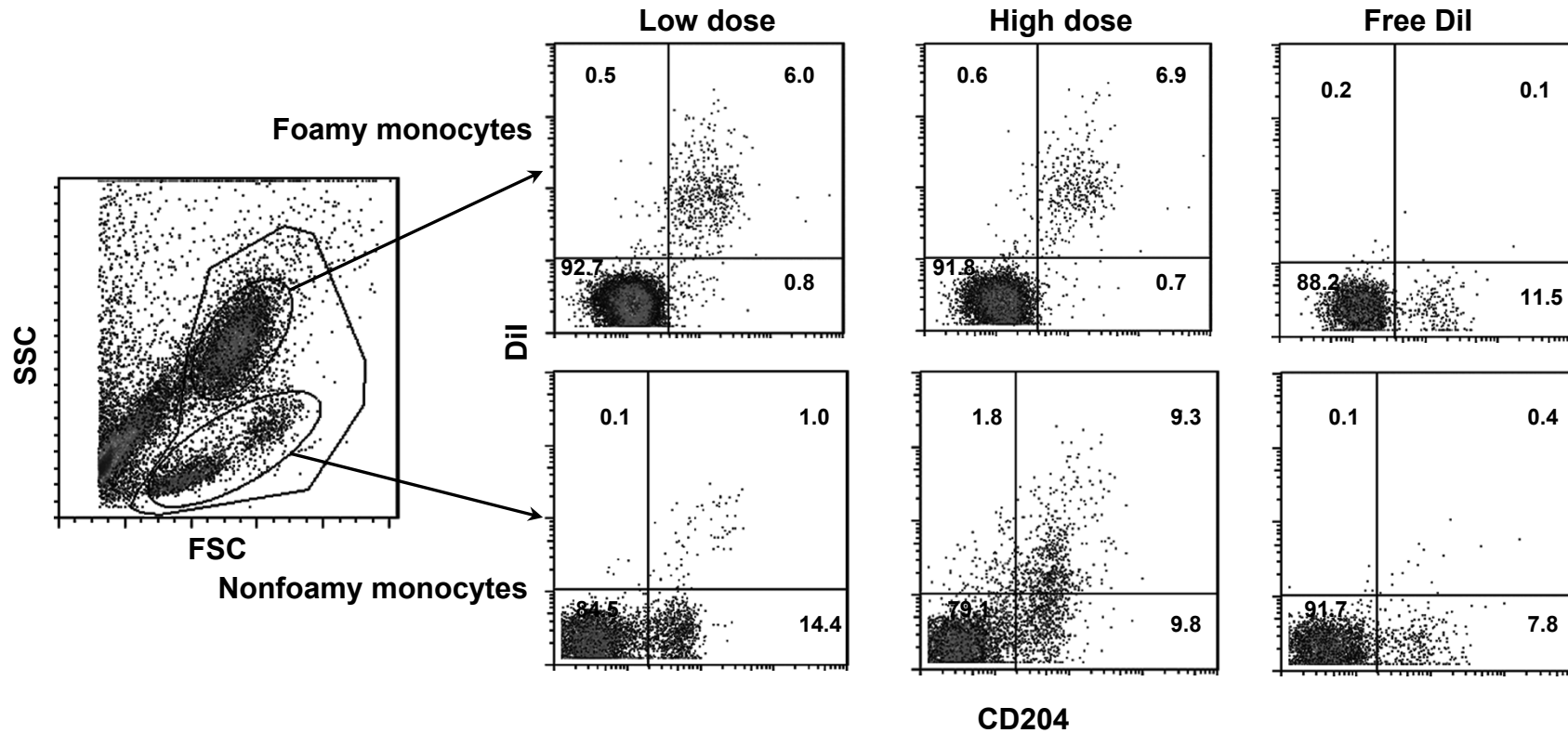
Immunohistochemistry staining for Mac-3



Supplemental Figure XI. CD11c^{+/+}/apoE^{-/-} and CD11c^{-/-}/apoE^{-/-} mice were fed WD for 3 weeks. Aortic sinus atherosclerotic lesion size, as indicated by oil red O staining, and lesional macrophage content, as indicated by immunohistochemistry staining for Mac-3, were examined. Magnification of the representative images was 20X. n=3–4 mice/group.

Supplemental Figure XII

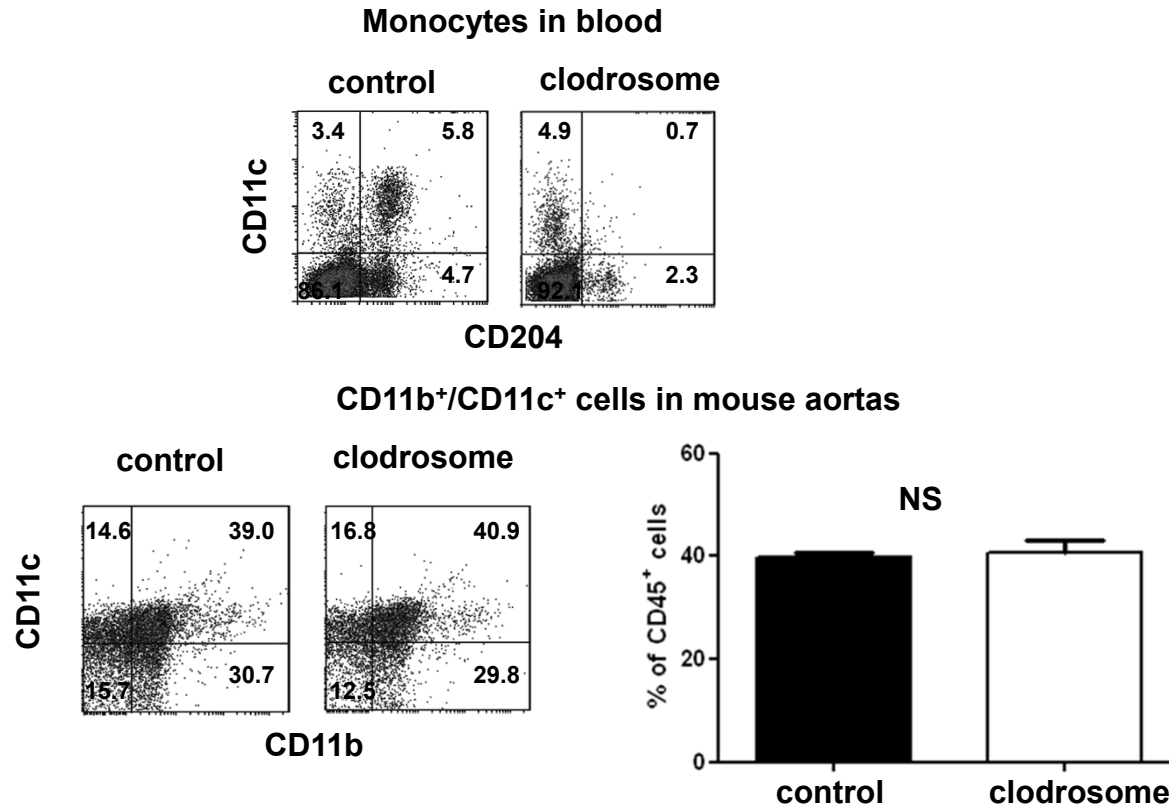
Uptake of Dil-clodrosome by blood monocytes in apoE^{-/-} mice on WD



Supplemental Figure XII. A bolus of “low-dose” (0.1 ml/mouse after 1:5 dilution) or “high-dose” (0.2 ml/mouse undiluted) Dil-clodrosome or free Dil was intravenously injected into apoE^{-/-} mice on WD. At 3 hours after injection, blood monocytes were examined by flow cytometry after staining for CD204. Representative data are presented from 3 mice in each condition with similar results.

Supplemental Figure XIII

Effects of a bolus injection of clodrosome on blood monocytes and aortic CD11b⁺/CD11c⁺ cells in apoE^{-/-} mice on WD



Supplemental Figure XIII. A bolus (0.2 ml/mouse) of clodrosome or PBS (control) was intravenously injected into apoE^{-/-} mice on WD (3 weeks). At 22 hours after injection, blood monocytes and CD11b⁺/CD11c⁺ cells in aortas were examined by flow cytometry. n=3 samples/group.

Supplemental Table I. Nutrition facts of special diets

	Western diet (WD)	High-fat diet (HFD)	High-cholesterol diet (HCD)
Fat (% w/w)	Milkfat 21	Milkfat 21	Milkfat 5
SFA* (% w/w)	13.3	13.3	3.2
MUFA (% w/w)	5.9	5.9	1.4
PUFA (% w/w)	0.9	0.9	0.2
Cholesterol# (% w/w)	0.2	0.05	0.2
Carbohydrate (% w/w)	49	49	58.2
Protein (% w/w)	19.5	19.5	26.4

*SFA: saturated fat; MUFA: monounsaturated fat; PUFA: polyunsaturated fat.

#This indicates cholesterol content from milkfat (0.256%) only for HFD, or cholesterol from milkfat plus additional sources for WD and HCD.

References

1. Mak S, Sun H, Acevedo F, Shimmin LC, Zhao L, Teng BB, Hixson JE. Differential expression of genes in the calcium-signaling pathway underlies lesion development in the LDb mouse model of atherosclerosis. *Atherosclerosis*. 2010;213:40-51.
2. Wu H, Gower RM, Wang H, Perrard XY, Ma R, Bullard DC, Burns AR, Paul A, Smith CW, Simon SI, Ballantyne CM. Functional role of CD11c⁺ monocytes in atherogenesis associated with hypercholesterolemia. *Circulation*. 2009;119:2708-2717.
3. Hoebe K, Georgel P, Rutschmann S, Du X, Mudd S, Crozat K, Sovath S, Shamel L, Hartung T, Zahringer U, Beutler B. CD36 is a sensor of diacylglycerides. *Nature*. 2005;433:523-527.
4. Galkina E, Kadl A, Sanders J, Varughese D, Sarembock IJ, Ley K. Lymphocyte recruitment into the aortic wall before and during development of atherosclerosis is partially L-selectin dependent. *J Exp Med*. 2006;203:1273-1282.
5. Koltsova EK, Garcia Z, Chodaczek G, Landau M, McArdle S, Scott SR, von Vietinghoff S, Galkina E, Miller YI, Acton ST, Ley K. Dynamic T cell-APC interactions sustain chronic inflammation in atherosclerosis. *J Clin Invest*. 2012;122:3114-3126.
6. Wang J, Perrard XD, Perrard JL, Mukherjee A, Rosales C, Chen Y, Smith CW, Pownall HJ, Ballantyne CM, Wu H. ApoE and the role of very low density lipoproteins in adipose tissue inflammation. *Atherosclerosis*. 2012;223:342-349.
7. Jiang E, Perrard XD, Yang D, Khan IM, Perrard JL, Smith CW, Ballantyne CM, Wu H. Essential Role of CD11a in CD8⁺ T-Cell Accumulation and Activation in Adipose Tissue. *Arterioscler Thromb Vasc Biol*. 2014;34:34-43.
8. Potteaux S, Gautier EL, Hutchison SB, van Rooijen N, Rader DJ, Thomas MJ, Sorci-Thomas MG, Randolph GJ. Suppressed monocyte recruitment drives macrophage removal from atherosclerotic plaques of Apoe^{-/-} mice during disease regression. *J Clin Invest*. 2011;121:2025-2036.
9. Tacke F, Alvarez D, Kaplan TJ, Jakubzick C, Spanbroek R, Llodra J, Garin A, Liu J, Mack M, van Rooijen N, Lira SA, Habenicht AJ, Randolph GJ. Monocyte subsets differentially employ CCR2, CCR5, and CX3CR1 to accumulate within atherosclerotic plaques. *J Clin Invest*. 2007;117:185-194.